Impact of urban heat island mitigation measures on microclimate and pedestrian comfort in a dense urban district of Lebanon

Jeff Fahed, Elias Kinab, Stéphane Ginestet, Luc Adolphe

Impact of urban heat island mitigation measures on microclimate and pedestrian comfort in a dense urban district of Lebanon

Jeff Fahed[1], Elias Kinab[2], Stephane Ginestet[1,*], Luc Adolphe[3]

[1] LMDC, Université de Toulouse, INSA, UPS, France
[2] Lebanese University, Beirut, Lebanon
[3] LRA, Université de Toulouse, ENSA, France

Jeff Fahed, Dr. Eng. Lebanese University, Beirut, Lebanon

Elias Kinab, Associate Professor, Dr. Eng. Lebanese University, Beirut, Lebanon

Stephane Ginestet, Professor, Dr. Eng. LMDC, Université de Toulouse, INSA, UPS, France

Luc Adolphe, Professor, Dr. Eng. Arch., LRA, Université de Toulouse, ENSA School of Architecture, France

Impact of urban heat island mitigation measures on microclimate and pedestrian comfort in a dense urban district of Lebanon

Abstract

The interaction between microclimate and buildings is predominant in urban areas. Thus, the urbanization constitutes the main cause of UHI formation. During the last years, several studies exposed the critical effects of UHI in the Mediterranean climate. As a result, there is a need for sustainable systems and urban policies to reduce heat islands in urban areas. This paper aims to present the impact of some UHI mitigation strategies in a Mediterranean city, Beirut Lebanon. Numerical microclimate simulations of an existing Lebanese district of Dora in Beirut, are performed using ENVI-met software. The study focuses on the potential of UHI mitigation scenarios to create freshness in summer conditions. The strategies are based on the increase of green surfaces, on the installation of water spray and fountains, and on the increase of the albedo of the facades and roofs of the buildings. A focus is carried out on white models, dealing with the albedo modification of roads and buildings. The effect of the proposed strategies on the pedestrian comfort is also evaluated by using the physiologically equivalent temperature PET. Results pointed out that implementation of water features contributes to a significant reduction of ambient temperature reaching a maximum of 5°C. In term of outdoor thermal comfort, the results showed the important role of green areas on the improvement of pedestrian comfort during daytime. Finally, this research supports a set of actions that could be helpful for urban designer to create cool islands in the Lebanese neighborhoods.

1. Introduction

In 2018, 55% of the world's population lives in urban areas, and this percentage is expected to achieve 68% by 2050 [1]. This rapid urbanization affects the microclimate in the urban regions and will cause additional increase in air temperature. Then, the cities and urban areas will be much warmer than the surrounding rural areas; this phenomenon is known as the urban heat island "UHI", and is mainly related to the high absorbing urban materials, the characteristic of urban morphology and urban canyons, the lack of green spaces, and the production of the anthropogenic heat [2]. Luc Howard was the first who spoke about the UHI [3], mentioning that cities are hotter than adjacent rural zones. The studies of Chandler [4] [5] and specially Tim Oke [6] [7] allowed to define the characteristics of the urban heat islands and their effect on the cities. The heat island intensity ΔT_{u-r} defined by the temperature difference between urban and rural zones, can reach considerable value. According to [8], the temperature difference can range from

1

2 °C for a city of 1000 inhabitants to 12 °C for a megacity of several millions of inhabitants. The increase in temperature due to the UHI causes many implications especially on the energy consumption, pedestrian comfort, environment and human health [9] [10] [11] [12] [13]. Many studies have already shown that the increase in air temperature will lead to an increasing in the number of mortality. A study in the Netherlands, demonstrated how the ambient temperature affected the mortality during 1979-1997. The results show that for each degree increase in air temperature above the optimum, the total mortality increased by 2.72 % [14]. Health Canada stated also that in seven Canadian cities, when the average temperature exceeds the 20 °C, the relative mortality increases by 2.3 % for each degree increase in air temperature [15].

The urban heat island phenomenon has been the subject of several numerical and experimental studies carried out on Mediterranean cities where a dry summer climate is observed. For Greece, many studies have shown the effect of the UHI on the cities. According to the data collected from fixed urban and rural meteorological stations around the Athens basin for the period 1961-1982, the UHI intensity was up to 3 °C based on the minimum mean monthly air temperature [16]. [17] found that large-scale increases in the urban surface albedo, could lower air temperature by 2 °C. The effect of the UHI in small town of the western Greece was studied by [18]; they found that UHI was dominating at night and the average monthly UHI intensity in August 2010 reached 3.8 °C during the night while the highest instantaneous hourly intensity was 5.6°C. In addition, UHI was studied in various Italian cities. The study of [19] showed that UHI intensity in Rome reaches 2 °C in winter and 5.2 °C in summer. Other studies was developed showing the impacts of the UHI and stressful meteorological conditions on health problems in different Italian cities, such as Bologna [20] and Milan [21]. In 2015, the simulations of [22] for Venice mainland, revealed that adopting lighter materials and green permeable surface for the roof and the pavement, lead to a reduction of air temperature by 4 °C. The topic of UHI in Morocco was discussed by [23] presenting the influence of urban geometry on outdoor thermal comfort in Fez, using PET (Physiologically Equivalent Temperature) index. PET is based on the Munich Energy-balance Model for Individuals (MEMI), which models the thermal conditions of the human body in a physiologically relevant way. A comparison between extremely deep and shallow street canyon in Fez, showed that the deep canyon is more comfortable during the summer. The UHI effects have been also studied in France. The experimental study of [24] compared the measurements between an urban and a rural site in Paris, during winter of 1995. They indicate that heat island intensity varies between 0 °C and 6 °C, and the maximum value occur at 8:00 in the morning. The impacts of UHI mitigations strategies in Lyon were the subject of [25] study. [25] found that green facades are the most efficient scenario for reducing energy consumption, but these results are relative to the case studied and could be different for another urban configuration. The UHI in Spain was the subject of different researches. [26] highlighted that during the night, the city center of Barcelona was 2.9 °C warmer than the airport. In Madrid, a numerical study showed that modifications in the roof albedo and building materials properties lead to a reduction in the total energy consumption by 4.8 % and 3.6 %, respectively [27]. The UHI intensity is also quantified in Lisbon, Portugal. Alcoforado et al. [28] found that mean intensity of the nocturnal UHI in Lisbon varies from 0.5 °C to 4 °C. In Aveiro, a small city in coastal Portugal, the maximum value of heat island intensity reaches 7.5 °C [29].

2

It is clear that the consequences of the UHI are very critical especially that many cities will face challenges to reduce urban heat island intensity due to the rapid urbanization and the non-consideration of the UHI phenomenon in the urbanization planning. Therefore, the researchers and the planners have done many studies in the last years, to propose methods and strategies in order to mitigate the UHI effects. For example, Ouranos a research consortium on regional climatology created in 2001 [30], presents strategies to better adapt to climate change based on several elements such design of optimal technologies and modification and adaptation of policies and standards. A French national research project called "UCI - urban cool island project" discussed a set of reasoned measures to mitigate UHI effects in Montaudran district of Toulouse. Results pointed out the important impact of water features and green spaces on the mitigation of heat islands, notably in daytime [31]. The application of greenery has used in a certain number of studies to mitigate UHI intensity. Results have indicated the cooling effect of increasing the vegetative cover in urban areas and adding green roofs [32] [33] [34] [35]. More recently a research in United states showed that green roofs have a marginal effect on UHI mitigation in high-rise urban morphology, while increasing the grass and tree coverage ratio were effective, especially in hot climates [36]. Several studies reported that modifying surface albedo may mitigate UHI in urban spaces [37] [38] [39]. However, the usage of high albedo materials has shown some negative effects on the pedestrian microclimate by causing outdoor discomfort [15]. The cooling effect of water features in urban landscapes of Rotterdam-Netherland has been studied by Montazeri et al [40]. The results of the study showed that a water spray system at height of 3m, contributes to a maximum temperature reduction of 7°C at pedestrian height.

The interest of this research is to study the UHI in a compact existing district that need rehabilitation and not comparison between regions with different morphology. The urban fabric in Beirut is very heterogeneous and the density varies between different districts and regions. "Dora", a suburban region in the north east of Beirut, is chosen in our study. This city is characterized by a high urban density with a low percentage of green areas, having industrial, commercial and residential zones. We note also the absence of fountains and water bodies in public spaces. In summary, Dora currently needs urban cooling systems to mitigate the negative impacts caused by urban heat islands.

2. Methodology

For Lebanon, a country of western Asia, few studies on the UHI have been carried out. Lebanon is a small country occupying 10452 km^2 of total surface area, with total population of 6,082,357 [41]. 87 % of the population live in the urban zones and cities [42]. It is obvious that the population density in the urban zones is very high. The capital Beirut is one of the highest urban density between the Middle Eastern cities, with an estimated value of 21000 inhabitants per square kilometer [43]. According to the land use study prepared by the "National Land Use Mater Plan" [44], the capital Beirut is also classified as an artificial territory, since the percentage of the vegetation zones is very low compared to the city surface area. Figure 1 shows

that the increase in housing construction will be significant in the coming years; this increase is estimated 10 km^2 per year during the next years. Then, the constructed urban area will increase considerably causing high values of UHI intensity. Therefore, the study of the UHI phenomenon is very important in a dense city such Beirut. The Köppen-Geiger classification [45] [46], one of the most common climate classification systems in the world, is used to indicate the Climate of Beirut. Under Köppen-Geiger climate classification, Beirut is classified as "CSA". The main climate is warm with a dry and hot summer.
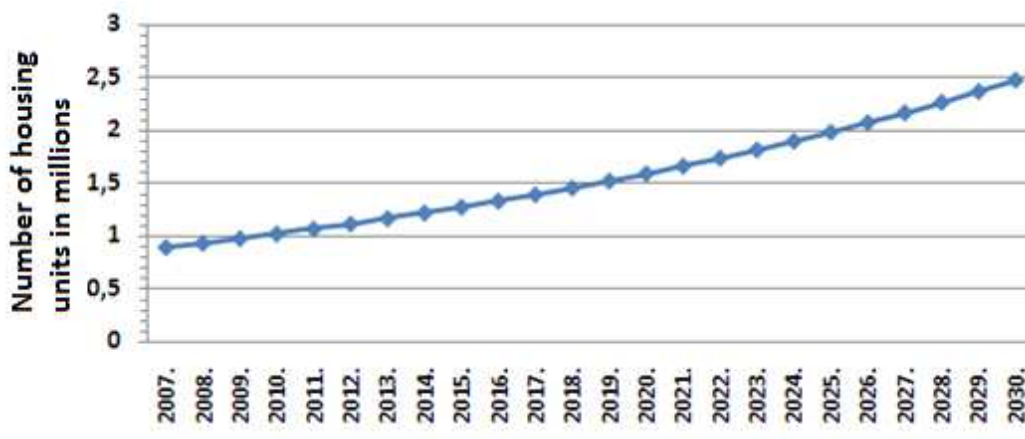

Fig. 1: Projection of the number of housing in Lebanon from 2007 to 2030 [47]

In the context of UHI in Lebanon, [48] used RCM model (Met Office Hadley Centre Regional Climate Model) to compare UHI in 3 different Mediterranean regions: Beirut, Athens and Alexandria. The results showed that the highest UHI intensity is in Beirut with a maximum value exceeding 7 °C. Furthermore, a global warming was observed in 1970 in 8 Mediterranean regions including Beirut [49], [50]. This warming was not uniform and according to Hasanean, this climate change may be the result of the urban heat islands and the accentuated urbanization. More recently, [42] used Town Energy Balance "TEB" model to study the effects of urbanization on the urban heat island in 5 regions of Beirut. In summer, the simulations results revealed that "Horsch Beyrouth" a region with large green area density, is 6 °C cooler than "Bachoura" a surrounding dense artificial region. The difference in temperature between these 2 regions is also observed in winter with a value of 2.5 °C.

The aim of this study, is to present and discuss the cooling potential of multiple UHI mitigations scenarios in a dense Lebanese district of Dora city. The scenarios are based on the increase of green surfaces, usage of high albedo material for urban surfaces and the implementation of water sources. A statistical analysis is used to show the relationship between the sky view factor (SVF) and the ambient and radiant temperatures. The sky view factor SVF is defined as the portion of the sky visible from a considerable surface [51]. Finally, the effect of the proposed strategies on the pedestrians comfort is also evaluated. To emphasize the objectives presented above, the following methodological steps were taken:

4

- Description of the exsiting district of Dora mentioning the dense morphology of the studied zone which is representative in the region.
- Definition of a set of mitigation scenarios based on urban variations of the initial model.
- Comparative analysis between the initial model and the proposed urban scenarios regarding the microclimate effects, using computational simulations.
- Evaluation of outdoor thermal comfort by comparing PET index of pedestrian itineraries of the base model and its variations.

2.1. Description of selected district

A district 210x350 m was selected to study the effects of several UHI mitigation strategies by simulating different scenarios. A satellite view of the selected district is shown in the figure 2. The district has a dense urban morphology that is repeated in most areas of the region, which explains the choice of the studied area dimensions. Most of the district buildings have a height between 15 m and 36 m. There are only three buildings with height less or equal to 10 m. An almost total absence of the vegetated surfaces and trees is observed in the studied area. The age of the buildings exceeds 25 years. The exterior walls consist of hollow blocks with gray color, while the roofs are made of concrete slabs non insulated (grey color). The studied area consists of 50 buildings and the distribution of district areas is shown in table 1. The width of secondary streets separating two neighboring buildings is very small, and does not exceed 5 m in some cases.

Fig. 2: Satellite view of the selected district, Dora area. Source: Google Earth. The red quadrilateral corresponds to the studied zone.

Table 1: Percentage of land surface coverage

Case of study, district Dora	Buildings	Road asphalt	Concrete pavement	Vegetation coverage	Total
Surface (m^2)	24875	46228	2175	222	73500

Percentage (%)	33.84	62.9	2.96	0.3	100

2.2. UHI simulations

ENVI-met 4, a three dimensional microclimate model [52] was used for numerical simulations. The modeling tool Envi-met, developed by M.Bruse, allows realistic microclimate simulation at the district scale due to its ability to integrate a large number of physics phenomena such the air flow between buildings, the impact of vegetation and water surfaces urban heat islands, and the exchanges between soil surfaces and buildings walls [53]. The effect of bioclimatology and pollutants emissions is also integrated in the model. Wind speed, air temperature and humidity are calculated using the non-hydrostatic incompressible Navier-Stokes equations and the advection convection equation. For the atmospheric turbulence, ENVI-met uses a 1.5 order turbulence closure model. The model is based on the work of Mellor and Yamada [54] and adds two additional equations for turbulence E and its dissipation (ε) [52]. The temperature of the ground surfaces is calculated from an energy balance taken into consideration the net radiative energy fluxes, the turbulent fluxes of heat and vapor, and soil heat fluxes. The calculation of the surface temperature of walls and roofs is based on the 3-node model allowing the energy balance calculation in transient state [52]. The differential equations in the model are solved on a staggered grid system using the finite difference method. The three-dimensional advection-diffusion equations are de-coupled using the Alternating Directions Implicit (ADI) method in combination with an upstream advection scheme. This scheme implies a relatively high numerical diffusion but allows a quick and implicit solution of the equations [55]. ENVI-met has a typical spatial resolution between 0.5 m and 10 m and time steps between 1 and 10 s.

For the mesh selection, the height of the grid in ENVI-met must be at least twice the maximum height of buildings. Since the district dimensions are 210x350 m with a maximum buildings height of 36 m, the only available predefined mesh version in ENVI-met that meet the requirement is 150x150x35. Therefore, the calculation domain grid dimensions (x,y,z) used in the simulations are 105x140x30 pixels, with each pixel corresponds to a reduced resolution 2m x 2.5m x 2.5m (dx = 2 m, dy = 2.5 m, dz = 2.5 m). The horizontal spacings dx and dy are constant for all grid cells. For the vertical grid, all grid cells have the same height dz except the lowest grid cell which is divided into five sub grid cells so that the vertical extension of these grid cells is 0.2 x dz [52]. The 3D model and the location of the 15 selected receptors are shown in the figure 3. Receptors are virtual "array sensors", that allow to get information about physical parameters evolution (T, RH, wind speed, e.g.) at different height. The receptors are implemented in 3 different subareas with different building densities: zone 1 includes receptors (1, 2, 3), zone 2 includes receptors (4, 5, 6, 7, 8), and zone 3 includes receptors (9, 10, 11 ,12, 13, 14, 15). The way of installation of receptors covers the whole district taken into consideration the different morphological characteristics.
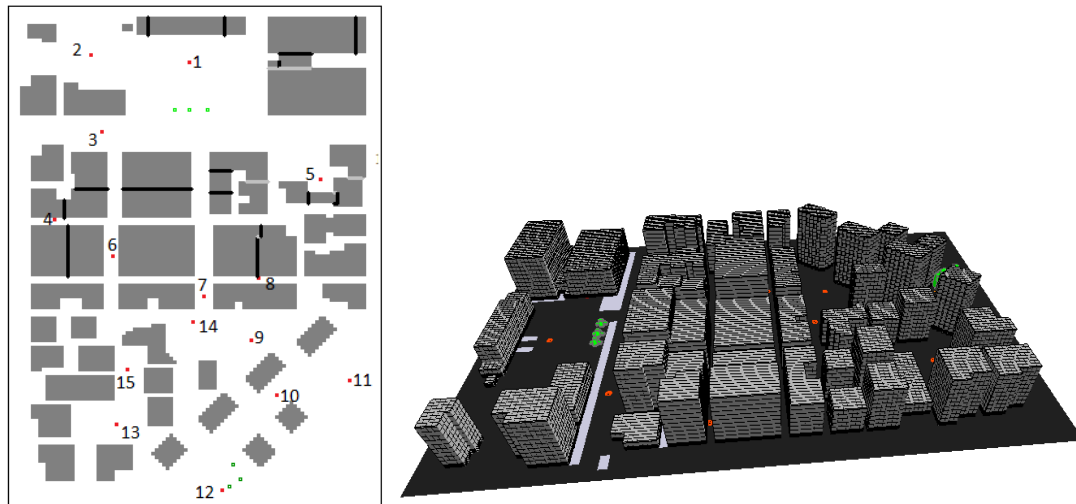
6

Fig. 3: 2D model of Dora district with the 15 selected receptors created with ENVI-met (left), 3D model of Dora district created with ENVI-met (right)

The microclimatic simulations were carried out for a hot summer day and for a period of 24 hours. The starting time chosen for the calculation is 7:00 am of the 9th of July. Since there are no meteorological stations in the Dora region, the choice of initial conditions is based on data available from Beirut Golf Station, year 2015 and AUB (American University of Beirut) Station, 1996 and 1997. The two mentioned stations are installed in urban areas. The radial distance between Dora and AUB is around 7 km, while this distance is about 8 km between Dora and Beirut Golf station. For the initial input parameters, we consider a wind speed of 1 m/s at height of 10 m, and a constant wind direction at all level with a value of 245° with the north direction. Indeed the value of the wind speed is variable in the summer season and reaches a minimum value of 1 m/s according to the available data of the two mentioned meteorological stations. This value in our calculation can often be detected in summer in a morphology like that of Dora because of the roughness and high urban density that lead to low wind speeds. The wind direction value corresponds to the mean direction of the wind observed at 7:00 in the two weather stations "AUB" and "Golf".
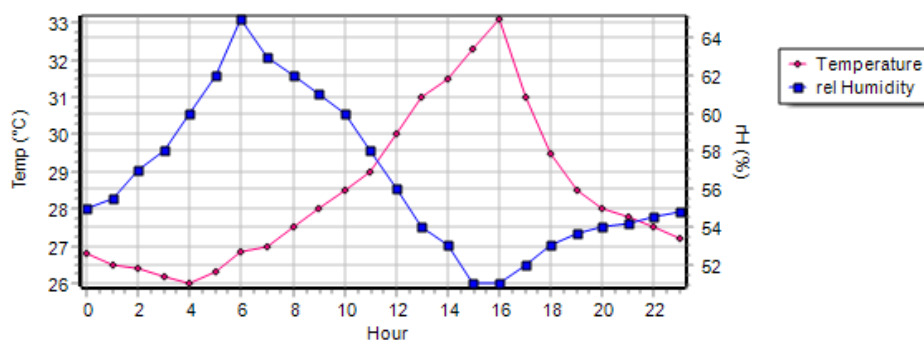

Fig. 4: Profiles of forced temperature and relative humidity using "forcing" function of Envi-met.

7

Fig. 5: Sub-model (part of the large model outlined in red) simulated to extract boundary conditions of air temperature and relative humidity.

ENVI-met "simple forcing" function was adopted to force the model to a temperature and relative humidity profiles during the simulation period. The simple forcing feature incorporated in ENVI-met is able to define the diurnal variation of the atmospheric boundary conditions: Temperature and relative humidity on an hourly basis. According to Huttner and Bruse, the simple forcing allows a better calibration [53]. The graph in Figure 4 shows the boundary conditions of temperature and relative humidity forced for the 24 hours of simulation. As we do not have weather data from a meteorological station near the Dora district, the forced values are extracted from a sub-model simulated with ENVI-met (red frame, Figure 5) and whose initial temperature is 26.9 °C and the relative humidity 65 % (average values of the two Golf and AUB stations). Indeed, the average values of air temperature and relative humidity around the sub-model buildings for each hour represent the forced values into the big district model. This method allows a higher precision of the boundary conditions since the morphology of the selected district is representative in the Dora region. For the initial soil temperature, a value of 20 °C at a depth of 2 m is used in the calculation. The dynamic time step used is 2s for solar angles lower than 50 degrees and 1 s for solar angles greater than 50 degrees. The general conditions of the simulations are summarized in table 2. Table 3 lists the albedo, the emissivity and the absorption of the surface material used in the simulations of the base model.

Table 2: General conditions for the simulations

Simulation date	Typical summer day, 9th/10th July
Simulation duration	24 h (from 7:00 am to 6:59 am)
Starting time	7:00 am
Wind speed in 10 m above ground	1 m/s
Wind direction	245° with the north direction
Relative humidity at 2 m	65%
Initial temperature of atmosphere	26.9 °C
Specific humidity at 2500 m	7 g/kg
Soil initial temperature	20 °C
Cover of low clouds (octas)	0
Cover of medium clouds (octas)	0
Cover of high clouds (octas)	0
Dynamic time steps	1-2 s

In order to compare the cooling potential of different UHI mitigation strategies against the "base model", five models were evaluated:

- Green model: addition of 7.1 % vegetation zones to the "base model" by planting trees and grass. ENVI-met three dimensional trees models are used in the simulation such as pines, olive trees, Citrus, palms and Albizia Julibrissin (table 4).

- Blue model: adding 5 water fountains with a continuous vertical emission height of 4 m, and water sprays P1/P2 with water jets at a height of 3.75 m from ground, as shown in the figure 7. P1 corresponds to a continuous line of water jet, while in P2 the distance between two consecutives sources corresponds to a pixel dx or dy. The hourly emission of the water sources is 5 $\mu g/s$ μm and the diameter of the particle is 10 μm.

- White model: installation of higher albedo materials for roads, pavements, buildings facades and roofs. The common asphalt used for roads has been replaced by asphalt with red coating. The light concrete is used for the pavements with an albedo of 0.8 instead of the ordinary concrete with an albedo of 0.4. The facades of the initial model are replaced by PVC facades with higher albedo (0.7 instead of 0.3). Roofs albedo are also increased by using Terracotta tiles. Table 3 resume the values of albedo chosen for the simulation of white model.

- White buildings model: the albedo of roofs and buildings façades is modified by using respectively PVC facades and Terracotta tiles. The roads and pavements are similar to the base model.

- Modified white model: Same as the white model with only modification of the buildings facades. The first five meters of the exterior walls are concrete with albedo 0.3, while the remaining walls are PVC as shown in the figure 8.

Table 3: Characteristics of the roads, pavement, walls and roof for the base case.

Surface	Exterior walls	Concrete Roof	Road asphalt	Concrete pavement
Albedo	0.3	0.3	0.2	0.4
Emissivity	0.9	0.9	0.9	0.9
Absorption	0.7	0.7	0.8	0.6

Table 4: Albedo of the modified surfaces in the "white" and white "buildings" models

	Albedo of roads	Emissivity of roads	Albedo of pavements	Emissivity of pavements	Albedo of facades	Emissivity of facades	Albedo of roof	Emissivity of roof
Base model	0.2	0.9	0.4	0.9	0.3	0.9	0.3	0.9
White model	0.5	0.9	0.8	0.9	0.7	0.9	0.5	0.9
White building model	0.2	0.9	0.4	0.9	0.7	0.9	0.5	0.9

Table 5: Foliage albedo of Trees in green model

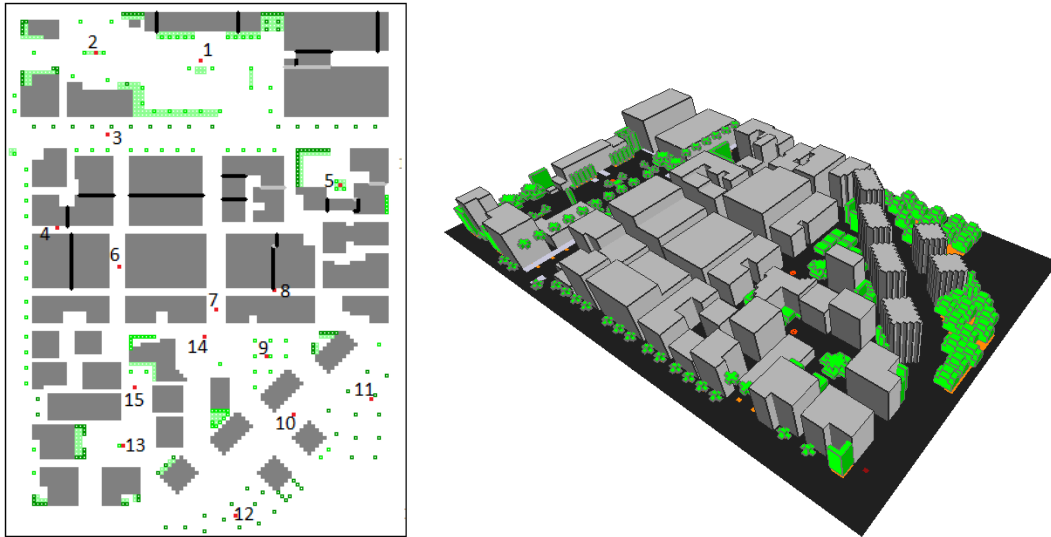| Trees	Albizia Julibrissin	Olive tree	Citrus	Pine	Palm
Foliage albedo	0.6	0.5	0.4	0.18	0.6

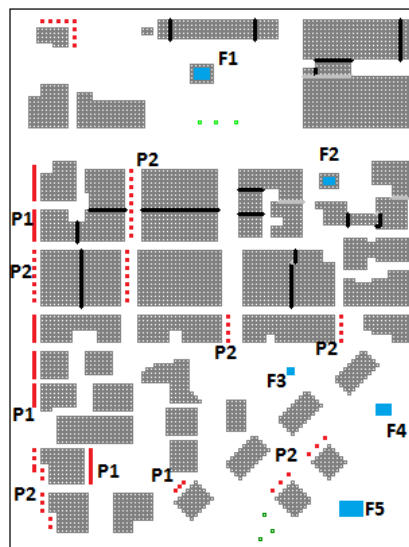*Fig. 6: 2D and 3D models of green scenario created by Envi-met*

Fig. 7: 2D Blue model created by Envi-met

Table 6: Area of the fountains installed in the "blue model"

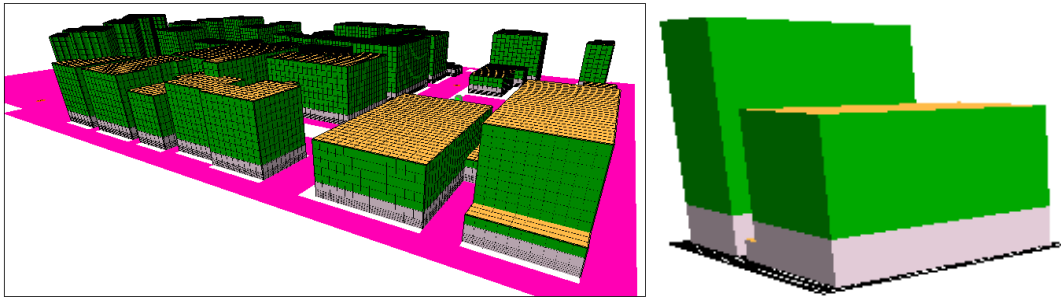| Fountain	F1	F2	F3	F4	F5
Area (m^2)	60	30	20	60	120

Fig. 8: Modified white 3D model showing the modification in the buildings facades (grey for concrete and green for PVC)

2.3.   Validation of Envi-met and comparison with meteorological data

The reliability and validation of Envi-met results were verified by several numerical studies comparing the results to the measured data [15] [56], [57], [58], [59], [60] [61] [62] . Fig. 9 shows an hourly comparison between meteorological measurement and simulation results. The weather data were derived from Golf station for the year 2015, and AUB station for the year 1996 and 1997. The simulation results correspond to the mean ambient temperature of the receptors implemented in the base model. The purpose of this comparison is to illustrate the variation of the ambient temperature of 3 zones with different urban morphology in the city of Beirut. The maximum Ta difference between the simulation and the measurement in Beirut Golf station is about 6.3 °C (at 4 pm of 9th July). Comparing the simulated temperature and the measurement of AUB station, a maximum temperature difference of 5.4 °C (at 3 pm of 9th July) and 4.4 °C (at 3 pm of 9th July) is respectively observed for the years 1996 and 1997. It is clear that simulated temperatures are warmer than those of stations. This increase in temperature is mainly due to the high percentage of mineralized materials in the Dora district. The observed difference could also be explained by inaccuracies in simulation input data assumed for surface materials, soil and vegetation properties. In addition, the simulation was carried out for cloud-free sky condition. The urban morphology could be also a reason for these discrepancies. The simulated site is a very dense neighborhood. In contrast, the AUB station is located in a university campus while Beirut Golf station is located in an area near the airport surrounded by vegetation and green areas.
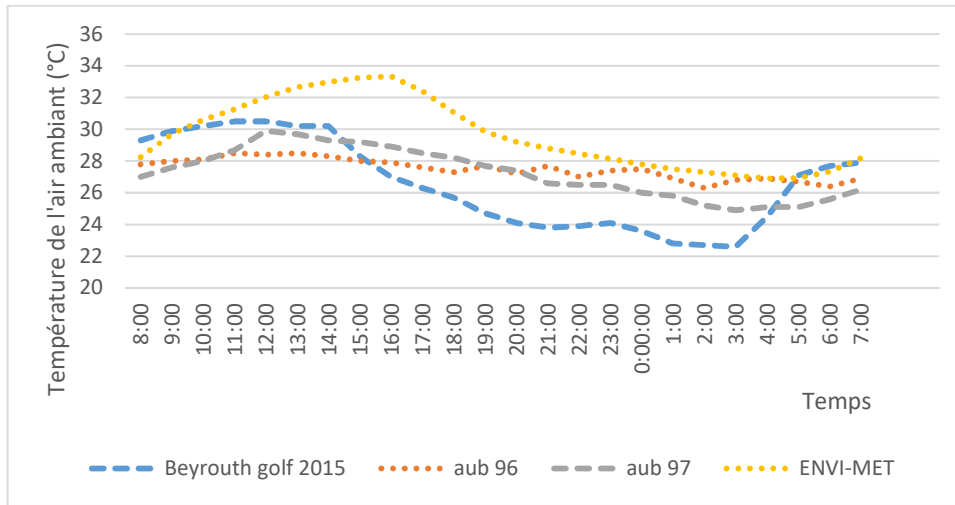
Fig. 9: Comparison of Envi-met results with measurement data.

3. Results

3.1. Effect of sky view factor

Statistical analysis relationships between SVF and the 2 microclimate parameters T_a (air temperature) and the mean radiant temperature T_{mrt}, is discussed in this section using the coefficient of determination R2. R2 is the square of correlation factor and its value varies between 0 and 1. A value close to 1 shows a strong correlation. As shown in the figure 10, the air temperature during the night is not strongly affected by the SVF, the coefficient of determination R^2 is low with a value of 0.195.
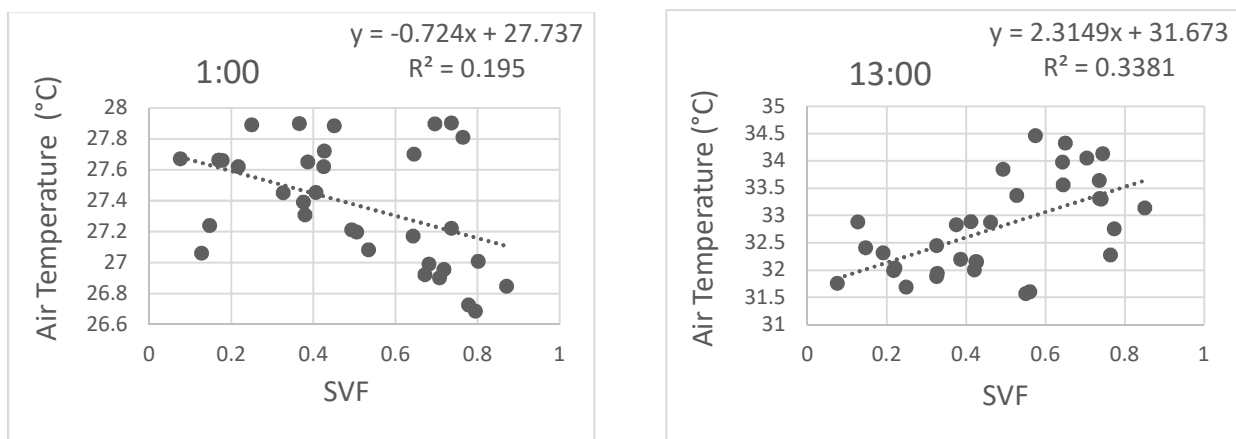

Fig. 10: The effect of SVF on air temperature at 13:00 (afternoon) and 1:00 (night). The data are collected from the receptors at 1.75 m above the ground.
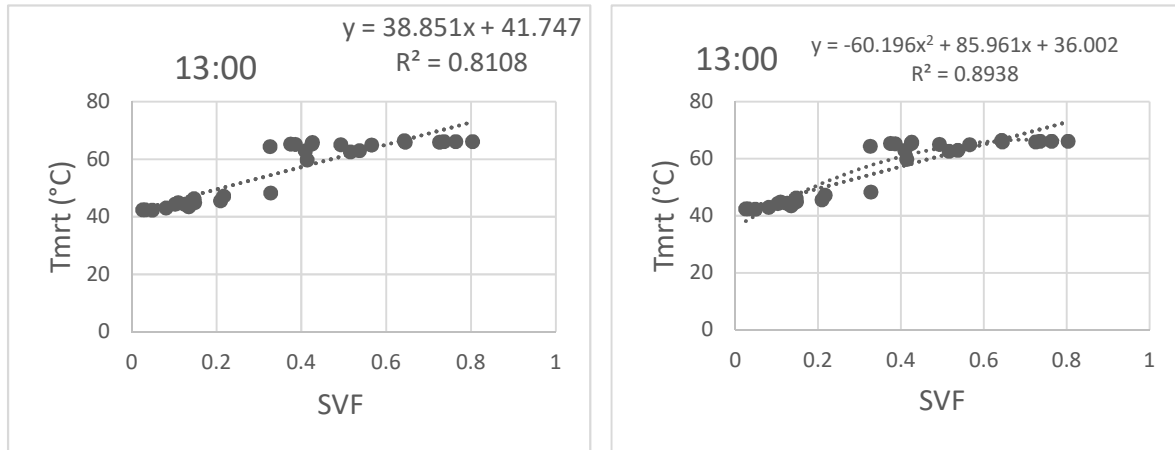
12

Fig. 11: The effect of SVF on the mean radiant temperature at 13:00 afternoon. The data are collected from the receptors at 1.75 m above the ground.

During mid-day, R^2 is higher with a value of 0.3381, showing that exposure to solar radiation due to high value of SVF induces an increase in T_a. The evolution of T_{mrt} as a function of the SVF during night and day, is illustrated in the figures 11 and 12. The results show that SVF affects much more the T_{mrt} during day and night than the air temperature, especially at noon (13:00) where R^2 reaches a high value of 0.81. As shown in the figures 11 and 12, the relationship between SVF and T_{mrt} appears to be more parabolic than linear; R^2 at night (1:00) reaches 0.6785 while 0.8938 during the day. Consequently, the results show that an urban zone with low sky view factor promotes a comfortable thermal environment in both daytime and at nighttime. A low SVF induces a reduction of exposure to solar irradiations and consequently a decrease in solar energy storage during the day. Therefore, in order to decrease the T_{mrt} and then to improve the exterior thermal comfort, shaded spaces (low SVF) and shadows produced by architectural elements or vegetation are required.
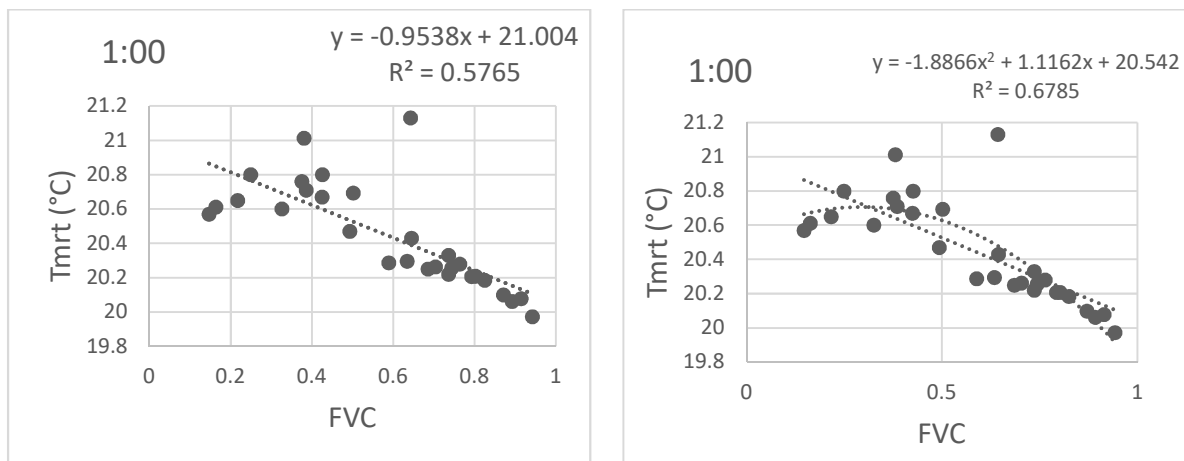

Fig. 12: The effect of SVF on the mean radiant temperature at 1:00 (night). The data are collected from the receptors at 1.75 m above the ground.

3.2. Effect of green model

The maps of figure 13 show the absolute difference air temperature between the green model and the base model at 13:00 pm during the day, and 1:00 am at night. The cooling effect of green scenario is observed during day and night; the cooling potential during the day is more important in the vegetated areas. At 13:00 pm, the maximum T_a reduction is 2.1 °C observed punctually near the green zones especially near the pines trees (pink spots, figure 12), while at 1:00 am the T_a is reduced by 0.5 °C. It is notable that the decrease in temperature is not only punctual but a spatial extension of freshness effect is observed during the day (around 0.5 °C) and during the night (around 0.3 °C).
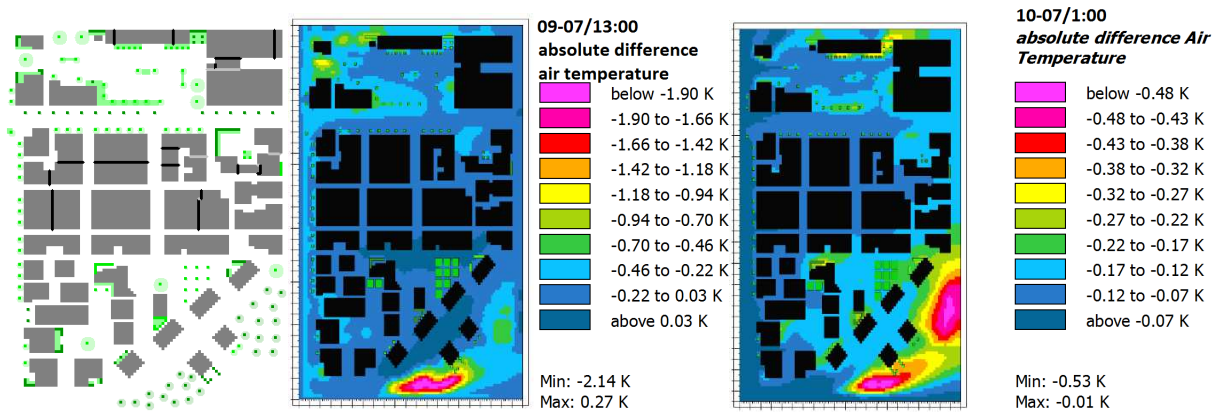

Fig. 13: Air temperature difference between the "green model" and "base case" during day (middle) and night (right).
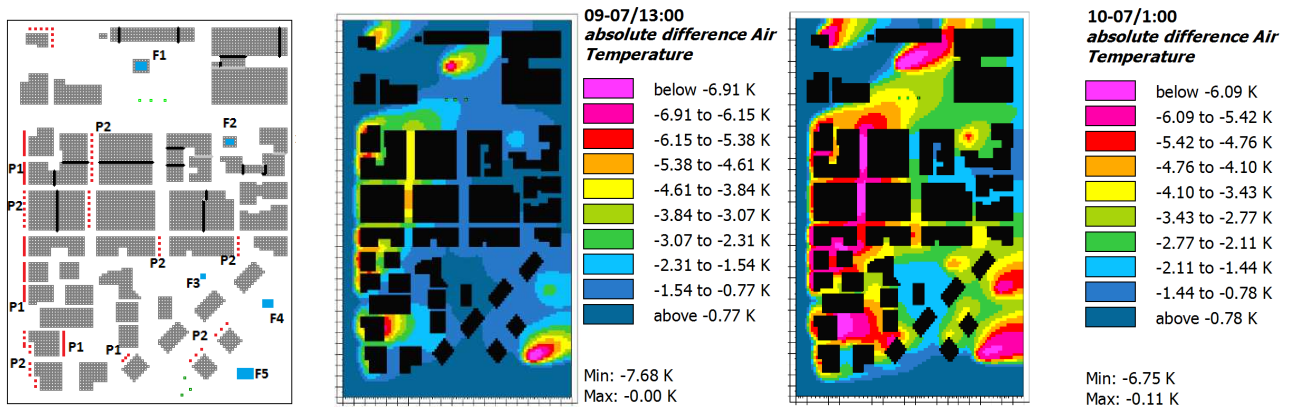

Fig. 14: Air temperature difference between the "blue model" and "base case" during day (middle) and night (right).
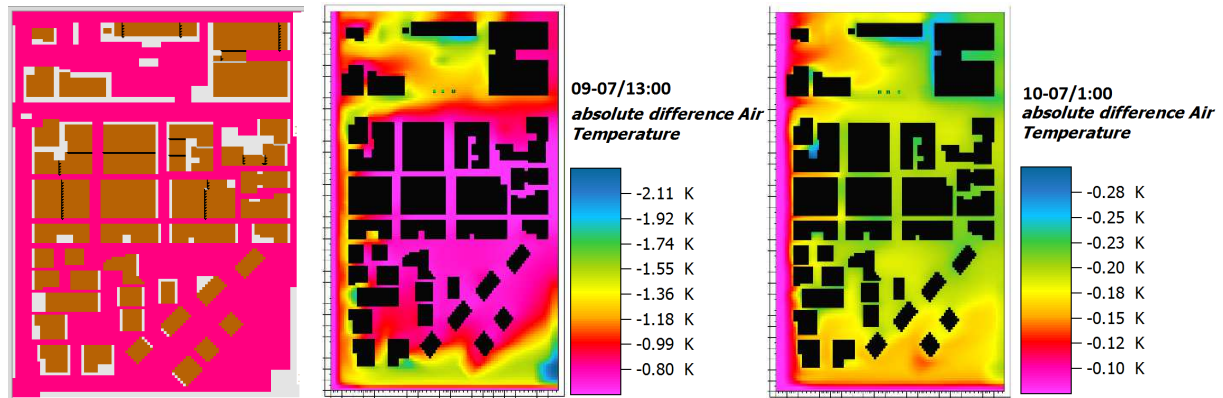
14

Fig. 15: Air temperature difference between the "White model" and "base case" during day (middle) and night (right).

The addition of vegetation in the green scenario affects also the specific humidity (g of water in kg of dry air) in daytime and nighttime; an increase in the specific humidity is observed. The maximum increase in the specific humidity is observed at noon to reach 1 g/kg compared to the base model. In addition, the specific humidity increase at midnight, and the highest difference is around 0.2 g/kg. The spatial extension of the effect of trees and vegetation on the humidity has been also identified. As expected, the addition of vegetated areas leads to an increase in the specific humidity due to the evapotranspiration phenomenon of the plants.

The results revealed that the mean radiant temperature T_{mrt} is also reduced during the day due to the shading effect of the trees. The T_{mrt} is calculated for a height of 1.75 m from ground, in order to analyze the results in terms of pedestrian comfort. The maximum reduction was observed around the pines and Allbizias trees; the difference reaches punctually around 30 °C at 15:00 pm. The addition of vegetated areas and trees creates a shading effect, and thus reduces the SVF. The reduction in SVF produces lower T_{mrt} and consequently generates an improved thermal comfort effect during summer.

3.3. Effect of blue model

As shown in the figure 14, the combination of fountains and water jets in the "blue model" contributes to a lower ambient temperature in most areas of the district during day and night, showing a spatial extension in the cooling potential. The effect of this scenario on T_a is important; punctually the maximum reduction of T_a is around 7 °C and is observed at 13:00 pm and 1:00 am. This reduction is due to the decrease in heat of the ambient air caused by the evaporation of the droplets ejected by the water sources. The freshness effect created by the "blue model" is not only observed where the water sources are placed, but also in the downwind areas and over a significant distance that can reach a hundred of meters. It is obvious that the effect of this scenario depends mainly on the direction of the wind. The average reduction of the ambient temperature in the downwind areas is around 2 °C at 13:00 pm as illustrated in the figure 12, and reaches 4 °C to 5 °C at 1:00 am. Thus, the cooling effect of the water sources is more important during the day. In term of air temperature, the blue model presents an effective solution to reduce the UHI effects. The water sprays of this model revealed an important

15

reduction of T_a in the narrow streets in the middle of the district where the implementation of fountains and vegetation is almost impossible.

The variation of the specific humidity is highly influenced by the blue scenario, due the amount of water evaporated in the air. As expected, the implementation of water sources leads to an increase in the air specific humidity in daytime and nighttime. This increase reaches a maximum local value of 3.5 g/kg at 13:00 pm and 3.3 g/kg at 1:00 am in the night. The spatial extension of the specific humidity variation in the downwind areas is also observed, and the maps appear similar to the maps of the air temperature variation. For the mean radiant temperature, the effect of the blue scenario is almost negligible. To conclude, the simulations have shown that fountains and water sprays mitigate the UHI effects by reducing daytime and nighttime ambient temperatures. On the other hand, these water sources increase the air humidity of which we will discuss the effect on the pedestrian comfort.

3.4.   White models

In this section, we discuss the effect of the albedo modification by studying 3 models: "White model", "White buildings model" and "Modified white model".

For the "White model", as can be seen from the maps of figure 15, high albedo surfaces for soil and buildings generate a cooling effect during the day over the entire area of the district. The maximum reduction is around 2.5 °C at 13:00 pm between the "White model" and the "initial model". During the night, the "white scenario" contributes to a small reduction of T_a with a maximum value of 0.35 °C at 1:00 am. During the day, it is clear that the cooling effect is more important on the main roads and the high SVF areas compared to the compact zones with low SVF. In fact, the temperature reduction is low in the areas around buildings in the center of the model where the SVF is very low. The cooling potential of "white scenario" depends on the urban configuration. In the case of Dora district, the "White model" presents an effective UHI mitigation strategy during the day. It should be noted that albedo value and the percentage of modified surfaces must be optimized for better results. Sub model test simulations showed that replacing 45.9% of the model areas by light concrete material (albedo 0.8) increased the ambient temperature around the building during the day [63]. For this, the choice of an albedo elevation of the district surfaces does not always reduce the ambient temperature due to the complexity of the physical phenomena and the interaction between the different elements of the urban volume.

The spatial distribution of the mean radiant temperature difference between "White model" and "Base model" at 13:00 pm, shows an increase in the T_{mrt} which reaches a maximum of 20 °C, figure 17. This maximum difference is observed in the areas just near the building (pink spots, figure 17) where the radiant heat is mostly reflected which leads to an increase in the radiant temperature. At night, the high albedo material produces a contradictory effect; at 1:00 am the T_{mrt} is slightly reduced with a maximum reduction of 1 °C. Indeed, the heat is easily dissipated by the high albedo material during the nighttime. In term of ambient temperature, "White model" allowed to reduce the T_a especially during the day, but this model negatively affects the outdoor thermal comfort by increasing T_{mrt}.

In the "White building model", high albedo buildings surfaces generate slightly cooler night compared to the base case, figure 16. On the other hand, the freshness effect of this scenario varies in the different zones of the district. In the center of the district, a slight decrease of Ta is observed reaching a maximum value of 0.15 °C at 13:00, while a slight increase in Ta has been generated in the western and southern zones. Contrary to expectations, our results showed clearly that the effect of "white building scenario" on Ta is almost negligible. Similar to "white model", the behavior effect of this scenario on the T_{mrt} is similar to the "white model" showing a contradictory effect between night and day. As expected, mean radiant temperatures during the day are higher than the base case due to the amplification of radiation exchanges caused by high albedo material. The maximum increase in Tmrt is observed near the building with a value of 6 °C in the afternoon. Contrarily, at night Tmrt is slightly decreased in the district to reach a maximum reduction of 1 °C. Therefore, the results presented previously showed that "white building model" may not constitute an optimal solution to create urban cool islands in terms of Ta and comfort. It is should noted that the effect of the "White building model" and "White model" on the specific humidity is negligible.

In order to reduce the increase in Tmrt caused by the high albedo surfaces of the "white model", the "modified white model" is used by modifying the albedo of building facades; the first five meters of the exterior walls are concrete with an albedo of 0.3, while the remaining parts of walls are PVC. The height of five meters is chosen in a way to have the largest possible façades area with high albedo, and to promote on the same time the outdoor thermal comfort. The modified model lead to the same cooling effect of the "White model" in term of ambient temperature. On the other hand, this new model leads to a decrease in the Tmrt compared to "white model"; the maximum Tmrt difference reaches 6 °C, figure 16. During the night, the maps showing Tmrt of "white" and "modified white" models are almost the same.
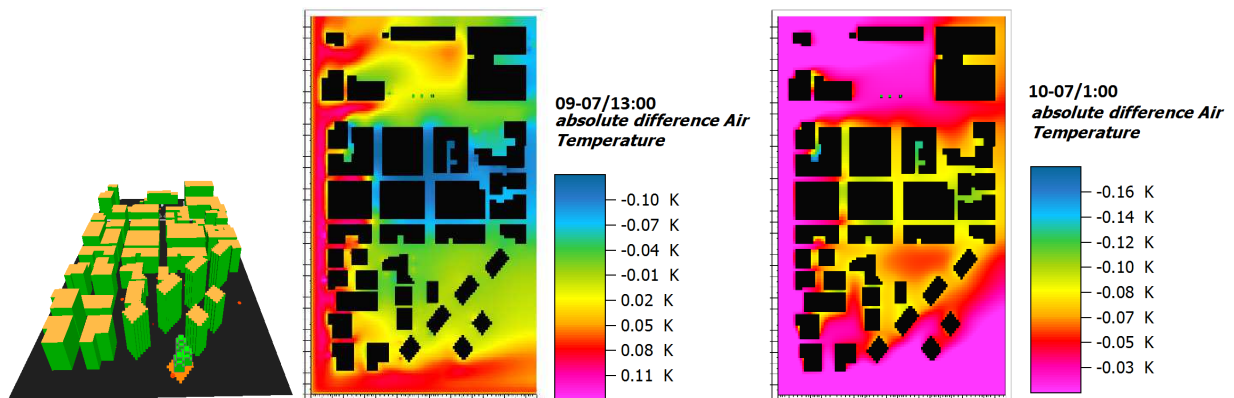

Fig. 16 : Air temperature difference between the "White building model" and "Base case" during day (middle) and night (right).
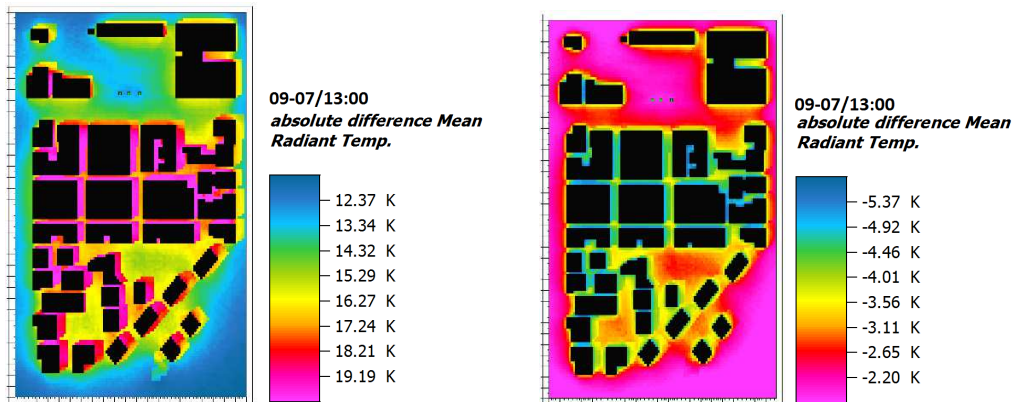
Fig. 17: T_mrt difference between the "white model" and "base case" during day (left). T_mrt difference between "modified white model" and "white model" during day (right).

3.5.   Outdoor thermal comfort and pedestrian itineraries

To create "sustainable cities", the design of external environment remains an essential element for urban activity. For that, an environment providing thermal comfort encourages the activity of pedestrians, tourists, bicycles and outdoor activities. In other words, outdoor thermal comfort can improve the quality of urban life and encourages the population to spend time in the streets and outdoor spaces that will be benefiting the cities in different levels: economic, social, touristic and environmental [64] [65] [66] [67]. The design of pedestrian comfort is mainly affected by the microclimate since the pedestrian is directly exposed to microclimate variables such as sunshine, wind speed, shading… The pedestrian thermal comfort in Dora district is analyzed using the physiological equivalent temperature PET. This index is suitable for the analysis of the outdoor thermal comfort [68] and used in different microclimatic researches [60] [69] [70] [71]. An itinerary inside the district is chosen to highlight the effect of the UHI mitigation strategies mentioned previously, on the outdoor thermal comfort. The itinerary is selected to diagonally cross the district, as shown in the figure 17.

For the calculation of PET, we considered the following assumptions: 35 years old man, 1.75 m tall, weighting 75 kg, walking at a speed of 1.21 m/s, total metabolism 164.49 W, with a clothing resistance of 0.5 clo.

The analysis of the outdoor comfort is studied at 16:00 pm a critical moment when the itineraries of the studied zone can be frequented by pedestrians and bicycles. It should be also noted that the hourly PET maps revealed that highest value of PET is detected at this time of the day hence the importance of analyzing the effect of the proposed UHI mitigation scenarios on outdoor comfort. The spatial distribution of PET difference between the initial model and the UHI limitation models (green, blue and white models) is shown in Fig. 18. Results showed that the shading effect caused by trees lead to the highest PET reduction reaching a local maximum of 20 °C. Unlike the green variant, the decrease in PET caused by the blue scenario is not only punctual but an extension in the downwind areas is observed. The maximum difference is about 5 °C . For the white model and as expected, the PET index is increased throughout the district and the map

18

appearance is similar to that of the mean radiant temperature. To better understand the influence of UHI mitigation measures on the pedestrian's thermal stress, an itinerary A-G (Figure 19) is chosen to study the variation of PET. The selected itinerary allows the pedestrian to pass the district diagonally. Likewise, the itinerary AG is used more during the day than during the night especially that the studied area is full of shopping, industrial centers and includes a hospital. On the contrary, the district does not include touristic sites causing low activity of pedestrian at night. By crossing the selected itinerary, the pedestrian passes through open spaces, narrow
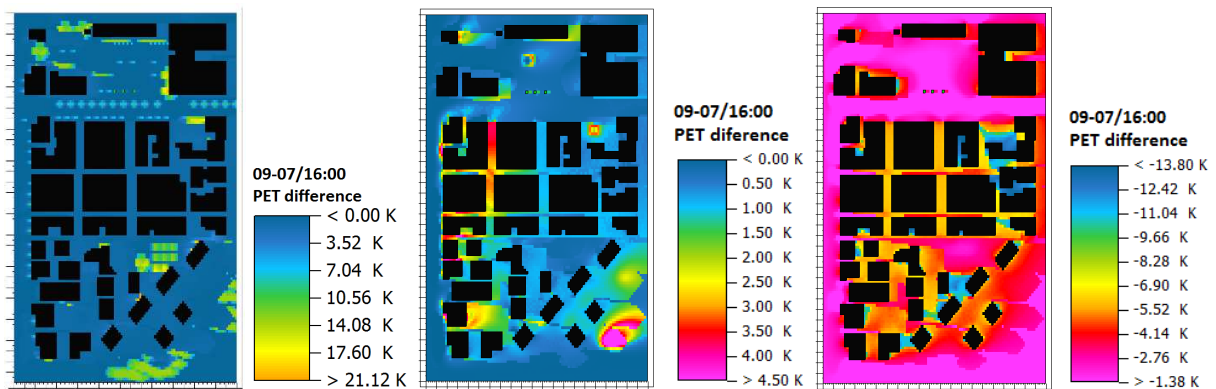

Fig. 18: PET difference between the "base case" and mitigation scenarios; "green model" (left), "blue model" (middle) and "white model" (left).
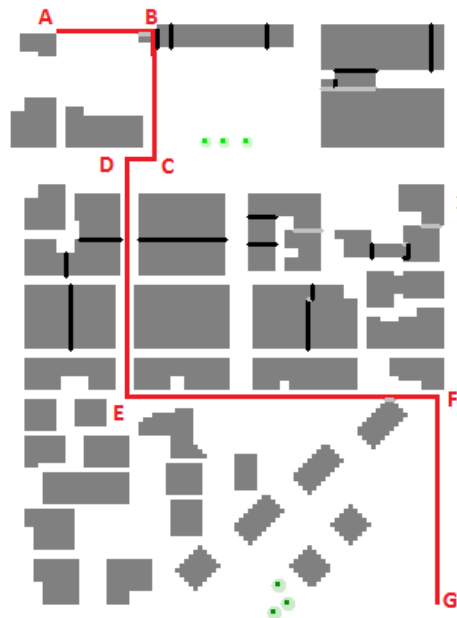

Fig. 19: A-G itenerary chosen for the calculation of PET

19

streets that separate buildings, main streets as well as under the trees of the green model, and around the water sources (fountains and sprays). PET is calculated at 1.75 m above the ground.

The graph in figure 20 shows the variation of PET for a pedestrian running the A-G itinerary. The results show clearly that the physiological equivalent temperature values along the A-G pathway are always above a threshold of 35 °C indicating that the pedestrian is always under thermal stress conditions. Figure 17 indicates that very high values of PET that exceed 50 °C are observed, especially in open spaces to reach a maximum of 57.4 °C. In these areas, the pedestrian is directly exposed to solar radiation, and the lack of shade provided by district elements such as trees and buildings are responsible for this discomfort. In the shaded area, especially in the narrow streets separating two tall buildings, the lowest values of PET are observed. These low PET values are observed mainly on D-F itinerary. The average PET in these shaded areas is around 36 °C with a minimum value of 35.7 °C. The sensation of discomfort and a strong heat stress are always observed on the itinerary AG, hence the importance of analyzing the potential of UHI mitigation strategies to decrease thermal comfort.
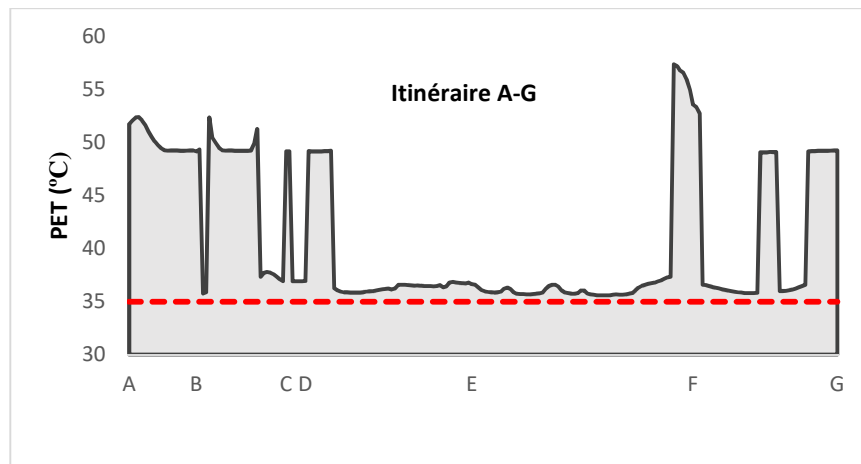

Fig. 20: Variation of PET in the case of the initial model.

For the green model, the variation of PET is illustrated in figure 21 in green color. The results show that PET values on the path A-G are smaller compared to the initial case values. The difference is not constant: a significant decrease of PET is observed under the trees whereas a small reduction of PET is noted where vegetation are absents. The punctually maximum reduction is around 14.3 °C and is observed on the path A-B when the pedestrian passes under the trees. This decrease is mainly explained by the shade effect caused by the trees preventing the pedestrians from being exposed directly to solar irradiation. Therefore, this reduction affects greatly the comfort of pedestrian who goes from a state of extreme heat stress (very hot) to a state of moderate stress (warm-hot sensation). Then the shade of trees creates an important island of freshness in term of external thermal comfort. On the D-F path where there is a total absence of green spaces, a small reduction of PET is observed and reaches PET values slightly lower than 35 °C.
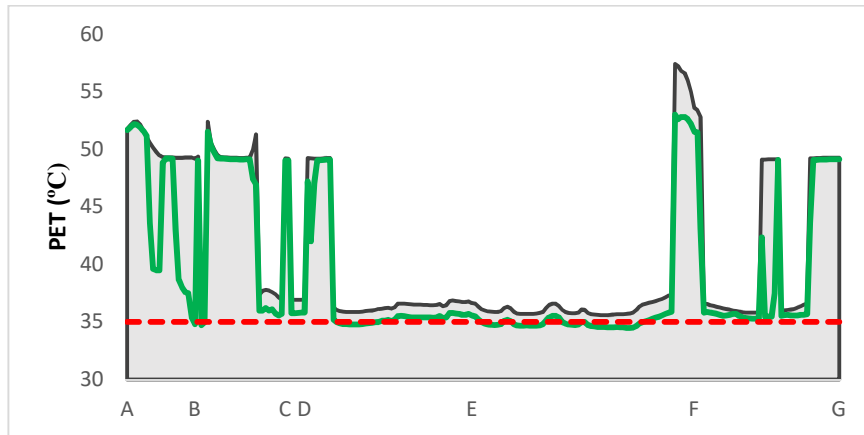
Fig. 21: variation of PET in the case of the green model.

For the blue scenario, pedestrians walk from A to G by passing near the water sprays and fountains. Figure 22, summarizes the influence of water sources on the PET in blue color. The results show that the PET along A-G is always lower than the PET of the initial model. For the path from A to C, the effect of this scenario is not significant. While for the C-G path, the PET was reduced due to the water sprays installed on the D-E path where the pedestrians pass directly below these sources, and due to the implementation of fountains near the E-G road. The maximum reduction achieved in this scenario is 4.3 °C leading to a decrease in PET from 36.6 °C to 32.3 °C. The importance of these values is the capacity of water sprays to improve the outdoor thermal comfort by reducing PET in the narrow streets where the implementation of trees is impossible. The extension of the fountains effect is also observable on the F-G path where a reduction up to 4 °C is obtained. On the other hand, in zones where PET values are high and exceed 50°C, the impact of this scenario is not important.
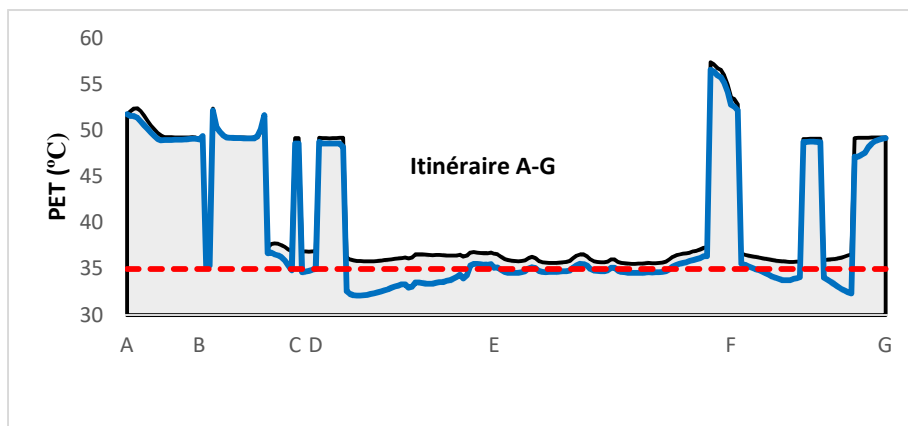

Fig. 22: Variation of PET in the case of blue model.

21

In the white scenario, the pedestrian follows the same path but is surrounded by high albedo surfaces: albedo of roads is 0.5, albedo of buildings facades is 0.7, and pavements albedo is 0.8. The PET variation in this scenario is shown in the figure 23. It is clear on this graph that the PET values of the A-G itinerary are higher than those of the initial model. The average PET on the A-G path is 3.9 °C higher than the initial model. The maximum deviation reaches 6.1 °C and is observed on the D-E path. For this scenario, the pedestrian is almost exposed to a condition of extreme stress. This variant caused additional discomfort even on the D-F path where the PET values of the initial model are the lowest and close to the threshold value. Indeed, solar radiations received by the district elements, are reflected by the high albedo materials producing an increase in the radiant temperature felt by the pedestrian.
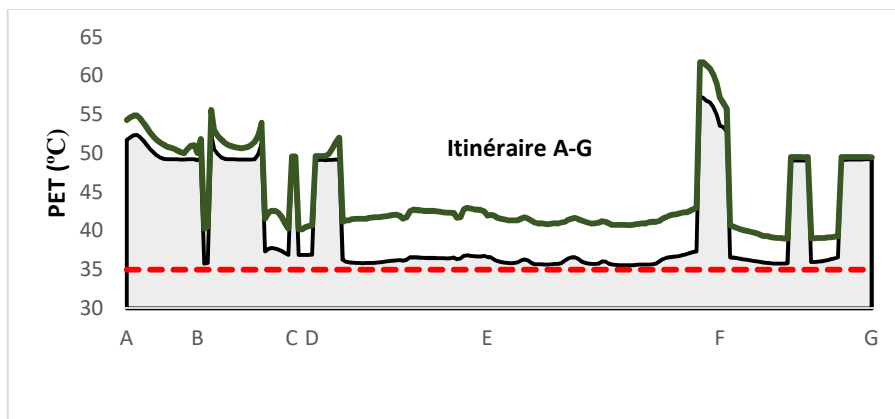

Fig. 23: Variation of PET in the case of white model.

For the white buildings model, figure 24 illustrates the variation of the PET on the A-G path compared to the initial model. With the exception of the D-F path, the results showed that PET is slightly increased due to the high facades albedo. On average, PET is increased by 1.3 °C and the maximum deviation is 2.3 °C observed on the D-E path. On this path, the pedestrians pass between two rows of high-rise buildings whose facades albedo is 0.7 causing multi-reflection of solar radiations. This model does not improve the pedestrian outdoor thermal comfort.

As mentioned above, the "White model" has led to greater PET compared to the initial model. The purpose of this part is to understand the behavior of the PET in the "Modified white model". The graph in figure 24 shows that physiological equivalent temperatures remain higher than the base case. In the "White" scenario, the above results have shown that PET is increased on average by 3.9 °C. The difference decreases in the "Modified model" from 3.9 °C to 2.8 °C. The maximum difference which was 6.1 °C in the "White" scenario, was also reduced to 4.3 °C. This model has improved pedestrian comfort comparing to the "White model", but still causes an increase in the PET compared to the initial model.
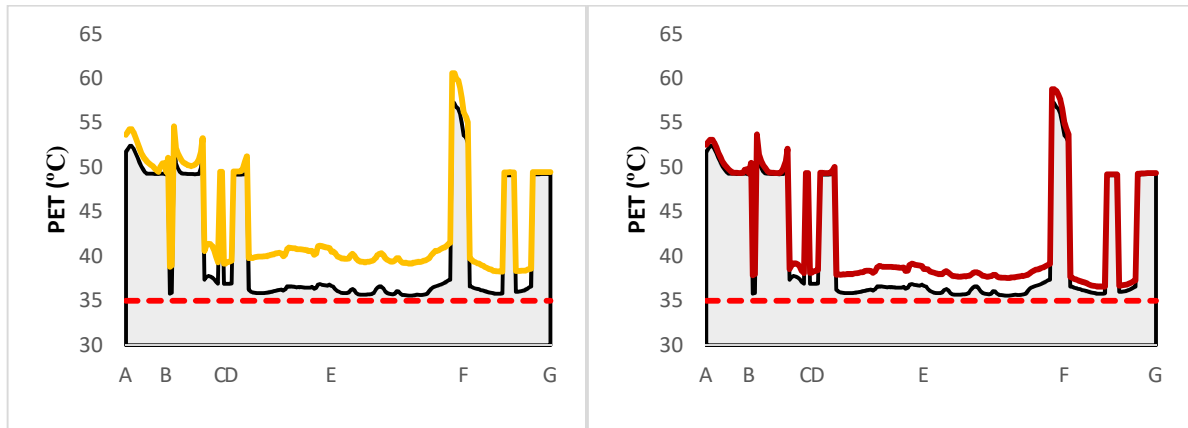
Fig. 24: Variation of PET in the case of the White buildings model (left) and in the case of the Modified white model (right) .

4   Discussion

The effects of the urban heat islands in the Mediterranean climate, especially in a dense city such as Beirut are expected to be increased and affecting the microclimate parameters and the outdoor thermal comfort. Therefore, urban planners and engineers are planning to propose UHI mitigation strategies in dense cities where the impacts are considerable.

The correlation between the sky view factor and the ambient temperature was firstly evaluated. The correlation between SVF and the mean radiant temperature is also studied. The results showed that the SVF affects the T_{mrt} more than the T_a. A high value of SVF leads to an increase in radiant temperature specially during sunny hours. Therefore, in order to create urban cool island by improving the outdoor thermal comfort, low SVF environment is proposed.

Vegetation, high albedo materials and water sources, can be considered as measures to be used by the planners to reduce the impacts of UHI. The simulations showed that vegetation lead to a freshness effect during day and night. T_a has been reduced to reach a maximum reduction of 2 °C during sunny hours when the vegetation spaces are increased only by 7 %.

The impact of high albedo materials on the UHI effects has been stated. For the "White building scenario" which relies on the use of a high albedo materials for the facades and roofs (PVC, albedo 0.7), it does not provide an effective solution for attenuation of UHI intensity with an insignificant impact on the ambient temperature in the case of the studied morphology "Dora district". On the hand, the "White" model which incorporates high albedo for pavement, roads and buildings envelopes, reduced the ambient temperature and reached locally a maximum of 2.5 °C around noon. At night, a slight reduction in temperature is observed. The disadvantage of the "White" and "White building" models is the important increase of the mean radiant temperatures caused by these models affecting negatively the outdoor comfort. Therefore, in order to avoid the significant increase in the T_{mrt} produced by the high albedo materials, a "Modified white model" is proposed. In this model, the first five meters of the exterior walls are concrete with low albedo (0.3). This model reduces the ambient temperature day and night (almost same effect as the "White model") and lead to the lowest possible increase in T_{mrt} compared to the other white

23

models. Consequently, it seems necessary to consider additional solutions (vegetation, water sources) to the modified model in order to improve pedestrians comfort.

The results showed that that the blue model based on the implementation of fountains and water sprays in the district, creates a significant freshness effect during day and night. In the areas near the water sources, the maximum temperature decrease reaches 7 °C with a remarkable spatial extension of the freshness effect in the direction of the wind. Under the conditions of the case studied, the blue scenario is the most effective in the reduction of air temperature.

In term of outdoor comfort, the PET graphs showed the effect of each scenario. Blue scenario lead to improve the pedestrians comfort throughout the 24 hours of simulations. The green model caused a reduction in the PET during the day due to the shading effect produced by the trees. A combination of these 2 scenarios (green and blue) would create additional comfort where the effects are added, and covers a larger area of the district with a PET close or below the threshold value. Indeed, in areas where it is difficult to add green surfaces such as narrow streets separating buildings, planners could incorporate water sprays in their design to improve outdoor comfort. The results have clearly shown that the white variants lead to additional external discomfort. Consequently, it is important to combine white variants with other scenarios such blue and green to obtain a suitable solution and to counterbalance the radiant effects of the high albedo materials.

The results of this work can be an important step in lunching guidelines for the development of existing cities in Lebanon specially Beirut and its suburbs. The proposed measures shown in this research, must be implemented and adopted by the urban planning, order of engineers and architects, municipalities and ministries specially in the absence of regulation and urban policies related to the adaptation of Lebanese cities to UHI and global warming.

5 Conclusion

In the context of Mediterranean climate, simulation studies have been carried out for evaluating the impact of proposed UHI mitigation scenarios in a dense district of Beirut. The choice of Beirut is justified by the limitation of UHI studies in this city. The software used for simulations is Envi-met. The effect of the SVF on the microclimate parameters T_a and T_{mrt} was evaluated using statistical study. It was demonstrated that mean radiant temperature is more affected by the SVF than the air temperature. The relation between SVF and Tmrt looks parabolic with high coefficient of determination R2 which reaches 0.9 at mid-day. In fact, higher SVF lead to an important increase in the mean radiant temperature. The proposed scenario used in the research was based on the implementation of vegetation, water sources and the modification of surfaces albedo. Adding 7 % of urban vegetation contribute to a decrease in the air temperature especially during the day reaching 2 °C. The blue scenario based on the implementation of fountains and water sprays, was the best strategy to mitigate UHI effect by reducing air temperature to reach punctually a maximum of 7 °C at 13:00 pm and 1:00 am. The originality of the blue model lies in the use of the misting effect of water features in ENVI-met. The results showed also the extension effect of freshness created by water sources that exceeds one hundred meter in the downwind areas. The average reduction in these areas is about 2°C at 13:00pm, while the

reduction is more significant during the night and reaches 5°C at 1:00 am. The impact of this scenario is almost observable in most areas of the district during daytime and nighttime. The usage of high albedo materials is critical and should be optimized since the models based on the replacement of low albedo material by higher albedo materials produced a contradictory effect by increasing the radiant temperature. Therefore, the white models should be combined by other models to improve the pedestrian comfort. At the end of this study, the impact of UHI mitigation strategies on outdoor comfort was evaluated by analyzing the variation of PET. Compared to the base model, a significant reduction in PET during daylight hours is observed in the green model. Under the trees of the green model, the PET could be reduced by 14.3°C at 16:00 pm in a summer day. The integration of water sources led to improve the comfort during day and night. The maximum reduction produced by the blue model at 16:00 pm is 4.3 °C. Conversely, strategies based on the usage of high albedo materials in the district, contributes to an important additional discomfort. Therefore, the usage of high albedo materials is not recommended in the spaces where the activity of the pedestrians is important.

Finally, this study constitutes an important step for the identification of an optimal case which is based on the aggregation of the strategies. The results of the blue scenario have proven their important potential for creating freshness islands, should constitute the body of new combination strategies.

Acknowledgments

References

[1]   "https://www.un.org/development/desa/en/news/population/2018-revision-of-world-urbanization-prospects.html," 2018. [Online].

[2]   T. Oke, D. Johnson, D. Steyn and I. Watson, "Simulation of surface urban heat island under 'ideal' conditions at night – part 2: diagnosis and causation," *Boundary-Layer Meteorology,* vol. 56, no. 4, p. 339–358, 1991.

[3]   L. Howard, The climate of London, Vols I-III., 1833.

[4]   T. Chandler, "Selected bibliography on urban climate.," *Tech. Note No. 155, WMO No. 276, World Met. Organiz., Geneva.,* p. 383, 1970.

[5]   T. J. Chandler, The climate of towns, Ch. 14 in the 'The Climate of the British Isles', Longman, pp. 307-329, London, 1976.

[6]   T. R. Oke, "Review of urban climatology, 1968-1973, Tech. Note NO. 134, WMO No. 383,

World Met. Organiz., Geneva, 132 pp.," 1974.

[7] T. R. Oke, "Review of urban climatology, 1973-1976, Tech. Note No. 169, WMO No. 539, World Met. Organiz., Geneva, 100 PP.," 1979.

[8] Oke, "Street design and urban canopy layer climate," *Energy and building 11(1),* pp. 103-113, 1988.

[9] EPA, "Heat Island Impacts," Available at: https://www.epa.gov/heat-islands/heat-island-impacts#main-content.

[10] A. Mohajerani, JasonBakaric and T. Jeffrey-Bailey, "The urban heat island effect, its causes, and mitigation, with reference to the thermal properties of asphalt concrete," *Journal of Environmental Management,* vol. 197, pp. 522-538, 2017.

[11] W. L. Filho, L. E. Icaza, V. O. Emanche and A. Q. Al-Amin, "An Evidence-Based Review of Impacts, Strategies and Tools to Mitigate Urban Heat Islands," *International Journal of Environmental Research and Public Health,* vol. 14, no. 12, 2017.

[12] A. Bhargava, S. Lakmini and S. Bhargava, "Urban Heat Island Effect: It's Relevance in Urban Planning," *Journal of Biodiversity & Endangered Species,* vol. 5, no. 2, 2017.

[13] R. Giridharan and R. Emmanuel, "The impact of urban compactness, comfort strategies and energy consumption on tropical urban heat island intensity: A review," *Sustainable Cities and Society,* vol. 40, pp. 677-687, 2018.

[14] M. M. Huynen, P. Martens, D. Schram, M. P. Weijenberg and A. E. Kunst, "The impact of heat waves and cold spells on mortality rates in the Dutch population," *Environ Health Perspect,* vol. 109 (5), pp. 463-470, 2001.

[15] Y. Wang, U. Beradi and H. Akbari, "Comparing the Effects of Urban Heat Island Mitigation Strategies for Tornoto, Canada.," *Energy and Building,* vol. 114, pp. 2-19, 2016.

[16] B. Catsoulis and G. Theoharatos, "Indications of urban heat island in Athens, Greece.," *J. Clim. Appl. Meteorol,* vol. 24, p. 1296–1302, 1985.

[17] A. Synnefa, A. Dandou, M. Santamouris, M. Tombrou and &. N. Soulakellis, "On the use of cool materials as a heat island mitigation strategy.," *Journal of Applied Meteorology and Climatology,* vol. 47, pp. 2846-2856, 2008.

[18] E. Vardoulakis, D. Karamanis, A. Fotiadi and G. Mihalakakou, "The urban heat island effect in a small Mediterranean city of high summer temperatures and cooling energy demands," *Solar Energy,* vol. 94, p. 128–144, 2013.

[19] V. Bonacquisti, G. Casale, S. Palmieri and A. Siani, "A canopy layer model and its application to Rome," *Science of the Total Environment,* Vols. 364 (1-3), pp. 1-13, 2005.

[20] I. Bertocchi, G. Fini, M. Rubolino and S. Tondelli, "Sustainability achievements in building regulations. The example of Bologna.," *Procedia Engineering,* vol. 21, p. 957–967, 2011.

[21] M. Pichierri, S. Bonafoni and R. Biondi, "Satellite air temperature estimation for monitoring the canopy layer heat island of Milan," *Remote Sensing of Environment,* p. 130–138, 2012.

[22] F. Peron, M. Maria, S. F. De and U. Mazzali, "An analysis of the urban heat island of Venice mainland," *Sustainable Cities and Society,* vol. 19, p. 300–309, 2015.

[23] E. Johansson, "Influence of urban geometry on outdoor thermal comfort in a hot dry climate: A study in Fez, Morocco," *Building and Environment,* vol. 41, p. 1326–1338, 2006.

[24] E. Dupont, L. Menut, B. Carissimo, J. Pelon and P. Flamant, "Comparison between the atmospheric boundary layer in Paris and its rural suburbs during the ECLAP experiment," *Atmospheric Environment ,* vol. 33, p. 979–994, 1999.

[25] E. Bozonnet, M. Musy, I. Calmet and F. Rodriguez, "Modeling methods to assess urban fluxes and heat island mitigation measures from street to city scale," *International Journal of Low Carbon Technologies,* vol. 10, no. 1, p. 62–77, 2013.

[26] M. C. Moreno-Garcia, "Intensity and form of the urban heat island in Barcelona," *International Journal of Climatology,* vol. 14, pp. 705-710, 1993.

[27] F. Salamanca, A. Martilli and C. Yagüe, "A numerical study of the Urban Heat Island over Madrid during the DESIREX (2008) campaign with WRF and an evaluation of simple mitigation strategies," *International Journal of Climatology,* vol. 32, no. 15, pp. 2372-2386, 2012.

[28] M. J. Alcoforado and H. Andrade, "Nocturnal urban heat island in Lisbon (Portugal): main features and modelling attempts," *Theoretical and Applied Climatology,* vol. 84, p. 151–159, 2006.

[29] O. Pinto and M. O. Manso, "The urban heat island in a small city in coastal Portugal," *International Journal of Biometeorology,* vol. 44, p. 198–203, 2000.

[30] C. Desjarlais, A. blondot and &. al, *S'avoir s'adapter aux changements climatiques, Montréal. Consortium sur la climatologie régionale et l'adaptation aux changements climatiques.Ouranus,* 2010.

[31] T. Martins, L. Adolphe, M. Bonhomme, B. Frédéric and e. al, "Impact of Urban Cool Island measures on outdoor climate andpedestrian comfort: Simulations for a new district of Toulouse, France," *Sustainable Cities and Society,* vol. 26, p. 9–26., 2016.

[32] T. Yokobori and S. Ohta, "Effect of land cover on air temperatures involved inthe development of an intra-urban heat island.," *Climate Research,* vol. 39, no. 1, pp. 61-73,

2009.

[33] E. Ng, L. Chen, Y. Wang and C. Yuan, "A study on the cooling effects ofgreening in a high-density city: an experience from Hong Kong," *Building and Environment,* vol. 47, p. 256–271, 2012.

[34] H. Yan, S. H. Fan, C. Guo, F. Wu, N. Zhang and L. Dong, "Assessing the effectsof landscape design parameters on intra-urban air temperature variability: thecase of Beijing, China," *Building and Environment,* vol. 76, no. 1, p. 44–53, 2014.

[35] M. Razzaghmanesh, S. Beecham and T. Salemi, "The role of green roofs in mitigating Urban Heat Island effects in the metropolitan area of Adelaide, South Australia," *Urban Forestry & Urban Greening,* vol. 15, pp. 89-102, 2016.

[36] H. Kim, D. Gu and H. Y. Kim, "Effects of Urban Heat Island mitigation in various climate zones in the United States," *Sustainable Cities and Society,* vol. 41, pp. 841-852, 2018.

[37] M. Taleghani, M. Tenpierik, A. v. d. Dobbelsteen and D. Sailor, " Heat mitigation strategies in winter and summer: field measurements intemperate climates," *Building and Environment,* vol. 81, p. 309–319, 2014.

[38] S. Saneinejad, P. Moonen and J. Carmeliet, "Comparative assessment ofvarious heat island mitigation measures," *Building and Environment,* vol. 73, p. 162–170, 2014.

[39] F. Salata, I. Golasi, A. d. L. Vollaro and R. d. L. Vollaro, "How high albedo and traditional buildings' materials and vegetation affect the quality ofurban microclimate. A case study.," *Energy and Buildings,* vol. 99, pp. 32-49, 2015.

[40] H. Montazeria, Y. Toparlar, B. Blocken and J. Hensen, "Simulating the cooling effects of water spray systems in urban landscapes: A computational fluid dynamics study in Rotterdam, The Netherlands," *Landscape and Urban Planning,* vol. 159, p. 85–100, 2017.

[41] Worldbank, "Urban Population (% of total). https://data.worldbank.org/country/lebanon," 2017. [Online].

[42] N. Kaloustian and Y. Diab, "Effects of urbanization on the urban heat island in Beirut.," *Urban Climate,* vol. 14, pp. 154-165, 2015.

[43] MOE/LEDO/ECODIT, " Lebanon State of the Environment Report," 2001.

[44] DAR-IAURIF, "National Physical Master Plan of the Lebanese Territory (NPMPLT) (Final). Prepared for: Council for Development and Reconstruction (CDR)," 2005.

[45] M. KOTTEK, J. GRIESER, C. BECK, B. RUDOLF and F. RUBEL, "World Map of the Köppen-Geiger climate classification updated," *Meteorologische Zeitschrif,* vol. 15, no. 3, pp. 259-263, 2006.

[46] H. Djamil and T. L. Yong, "Study of Köppen-Geiger System for Comfort Temperature Prediction in Melbourne City," *Sustainable Cities and Society,* vol. 27, pp. 42-48, 2016.

[47] A. Mourtada, "Energie, changement climatique et bâtiment en Méditerranée: Etude nationale Liban. Plan bleu.," 2010.

[48] M. McCarthy, "CIRCE (Climate Change and impact research: The Mediterranean environment).," 2009.

[49] C. Idso and S. Singer, "Climate Change Reconsidered: Report of the Nongovernmental Panel on Climate Change (NIPCC). The Heartland Institute," 2009.

[50] H. Hasanean, "Fluctuations of surface air temperature in the Eastern Mediterranean," *Theoretical and Applied Climatology,* vol. 68, no. 1-2, pp. 75-87, 2001.

[51] M. Colombert, "Contribution à l'analyse de la prise en compte du climat urbain dans les différents moyens d'intervention sur la ville. Thèse de doctorat de l'université Paris-Est," 2008.

[52] S. Huttner, "Further development and application of the 3D microclimate simulation ENVI-met. Thèse de doctorat de l'université Johannes Gutenberg, Mainz," 2012.

[53] M. (. Bruse, "Numerical modeling of the urban climate—a preview onEnvi-met 4.0.," in *The seventh International Conference on Urban Climate* , Yokohama, Japan, 2009.

[54] G. L. Mellor and T. Yamada, "Development of a turbulence closure model for geophysical fluid problems," *Review of Geophysics,* vol. 20, no. 4, pp. 851-875, 1982.

[55] M. Bruse, "ENVI-met 3.0 : Updated model overview," 2004.

[56] E. Lahme and M. Bruse, "Microclimatic effects of a small urban park in densely built–up areas: Measurements and model simulations. The European Commission in the 5th Framework Program under the contract EVK4-CT-2000-00041 (BUGS)," 2002.

[57] I. Ozkeresteci, K. Crewe and M. Bruse, "Use and Evaluation of the Envi-met Model for Environmental Design and Planning : an Experiment on Linear Parks. The 21st International Conference (ICC). Durban, South Africa, 10-16 August," 2003.

[58] C. Yu and W. Hien, "Thermal benefits of city parks," *Energy and Buildings,* vol. 38, pp. 105-120, 2006.

[59] A. Monam and K. Ruckert, "The Dependence of Outdoor Thermal Comfort on Urban Layouts. German-Iranian Research Project, Young Cities. www.univerlag.tu-berlin.de," 2013.

[60] A. Ghaffarianhoseini, U. Berardi and A. Ghaffarianhoseini, "Thermal Performance

Characteristics of Unshaded Courtyards in Hot and humid Climates," *Building and environmental,* vol. 87, pp. 154-168, 2015.

[61] M. H. Elnabawi, N. Hamza and S. Dudek, "Thermal perception of outdoor urban spaces in the hot aridregion of Cairo, Egypt," *Sustainable Cities and Society,* vol. 22, p. 136–145, 2016.

[62] F. Salata, L. Golasia, R. De Lieto Vollaro and A. De Lieto Vollaro, "Urban microclimate and outdoor thermal comfort. A proper procedure to fit ENVI-met simulation outputs to experimental data," *Sustainable Cities and Society,* vol. 26, pp. 318-343, 2016.

[63] J. Fahed, S. Ginestet, E. Kinab and L. Adophe, "Simulation and comparison of urban heat island mitigation strategies under Mediterranean climate: The case of Dora district, Beirut, Lebanon.," Edinburgh, 2017.

[64] A. Hakim, H. Petrovitch, C. M. Burchfiel, G. W. Ross, B. L. Rodriguez, L. R. White and e. al, "Effects of walking on mortality among nonsmoking retired men.," *New ENgland Journal of Medicine,* vol. 338, pp. 94-99, 1998.

[65] C. Hass-Klau, "Impact of pedestrianisation and traffic calming on retailing: A review of the evidence from Germany.," *Transport Policy,* vol. 1, pp. 21-31, 1993.

[66] J. Jacobs, "The death and life of great American cities. Harmondsworth: Penguin.," *Harmondsworth: Penguin.,* 1972.

[67] W. Whyte, "City: Rediscovering the center. New York: Doubleday.," 1988.

[68] P. Höppe, "The physiological equivalent temperature - a universal index for the biometeorological assessment of the thermal environment," *Int J Biometeorol. 1999 Oct;43(2):71-5.,* vol. 43, no. 2, 1999.

[69] N. Makaremi, E. Salleh, M. Z. Jaafar and A. GhaffarianHoseini, "Thermal comfort conditions of shaded outdoor spaces in hot and humid climate of Malaysia," *Building and Environment,* vol. 48, pp. 7-14, 2012.

[70] S. L. Heng and W. T. L. Chow, "How 'hot' is too hot? Evaluating acceptable outdoor thermal comfort ranges in an equatorial urban park," *International Journal of Biometeorology,* vol. 63, p. 801–816, 2019.

[71] F. Canan, I. Golasi, V. Ciancio, M. Coppi and F. Salata, "Outdoor thermal comfort conditions during summer in a cold semi-arid climate. A transversal field survey in Central Anatolia (Turkey)," *Building and Environment,* vol. 148, pp. 212-224, 2019.